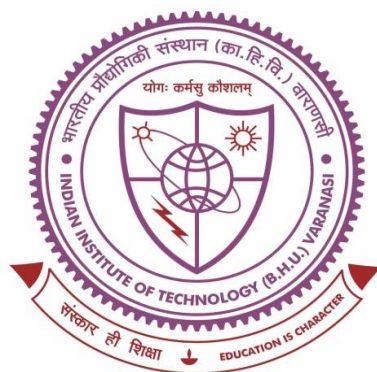


# PROJECTION APPROXIMATION FOR WEAKLY SINGULAR INTEGRAL AND INTEGRO- DIFFERENTIAL EQUATIONS



Thesis submitted in partial fulfillment for the  
Award of Degree  
**Doctor of Philosophy**

By

**Shiva Sharma**

**DEPARTMENT OF MATHEMATICAL SCIENCES  
INDIAN INSTITUTE OF TECHNOLOGY  
(BANARAS HINDU UNIVERSITY)  
VARANASI - 221005  
INDIA**

**Roll No.-13121009**

**2018**

# Chapter 5

## Collocation Method with Convergence for Generalized Fractional Integro-Differential Equations

---

---

### 5.1 Introduction

Fractional calculus describes many significant phenomena in science and engineering. The appearance of the fractional derivative in numerous applications can be found in the literature such as viscous-elasticity [126, 127], bioengineering [128], electrochemistry [115], electromagnetism [116], and more could be found in [43]. Most commonly used fractional derivatives in developing the theories and studying various applications are centred to the Riemann-Liouville and Caputo fractional derivatives. Some other derivatives of importance are also introduced and are known as Riesz- Riemann-Liouville, Riesz- Caputo fractional, and Grünwald–Letnikov derivatives. Authors are referred to see Ref. [43, 129, 116] for a concrete comprehension of fractional derivatives. There has been much developments on the analytical and numerical methods for solving the FIDEs in recent years. Some of them are described as follows: The most of existing numerical approaches like collocation method [43], least square method [72], pseudo spectral method [67] and hybrid collocation method [60] required adequately dense

---

*The contents of this chapter have been published in **Journal of Computational and Applied Mathematics** 342 (2018) 419–430.*

discretization of the domain. These methods follow the multistep process and it results in a large number of iteration which makes them low computationally efficient.

Here, in this chapter we consider the FIDEs (Eq. 5.1) defined in terms of a class of generalized derivative (B-operator, Chapter 1 Section 1.6.3) and thus name it as generalized fractional integro-differential equations (in short GFIDEs) and present the collocation approach to solve it. The Legendre polynomials are considered to approximate the unknown function in the GFIDEs. The convergence properties for GFIDEs of the presented approach is also proved. Some illustrative examples from literature varying the kernel in B-operators are considered to perform the numerical investigations. As B-operators reduces to Riemann Liouville fractional derivative, Caputo derivative, Riesz Riemann-Liouville derivative, Riesz-Caputo fractional derivative and many other fractional derivatives thus the method presented here could be easily applicable to FIDEs defined in terms of these derivatives.

## 5.2 Generalized Fractional Integro-Differential Equations

Here, we define GFIDEs in terms of B-operator Section 1.6.3 (Chapter 1) as follows,

$$(B_P^\alpha \gamma)(\xi) = (H\gamma)(\xi), \quad (5.1)$$

$$\gamma(0) = \gamma_0. \quad (5.2)$$

Here the right side of Eq. (5.1) is considered as,

$$(H\gamma)(\xi) = \varphi(\xi) + q(\xi) \gamma(\xi) + \int_0^\xi \rho(\xi, \eta) \mathcal{G}(\gamma(\eta)) d\eta, \quad (5.3)$$

and,

$$(B_P^\alpha \gamma)(\xi) = r \int_0^\xi \omega_{m-\alpha}(\xi, \eta) \mathfrak{D}^m \gamma(\eta) d\eta + s \int_\xi^1 \omega_{m-\alpha}(\eta, \xi) \mathfrak{D}^m \gamma(\eta) d\eta, \quad \alpha > 0. \quad (5.4)$$

In Eq. (5.1), we consider  $\mathfrak{S} = [0,1]$ , and  $m = 1$  in the B-operator. Here, functions  $\varphi(\xi)$  and  $q(\xi)$  are known functions belong to  $L^2(\mathfrak{S})$ . We assume,  $q(\xi) \neq 0$  for  $\xi \in [0,1]$ , and  $\gamma(\xi)$  is unknown function. The kernel  $\rho(\xi, \eta)$  in Eq. (5.3) is either smooth or weakly singular of the form

$$\rho(\xi, \eta) = (\xi - \eta)^{-\mu}, \quad 0 < \mu < 1. \quad (5.5)$$

We study Eq. (5.1) under the assumption that kernel  $\omega_\alpha(\xi, \eta) \in L^2(\mathfrak{S} \times \mathfrak{S})$  and  $\mathcal{G}$  is some linear or nonlinear operator.

We assume that Eq. (5.1) with Eq. (5.2) possess a unique solution for all real values of  $r$  and  $s$ . This equation is solvable for any real number  $r$  and  $s = 0$  or for any real number  $s$  and  $r = 0$ . The particular cases of this problem given by Eq. (5.1) has been discussed and solved in references [55, 61, 65, 68] with  $r = 1, s = 0$ . The aim of this chapter is to develop a numerical technique to solve the Eq. (5.1) with initial condition given by Eq. (5.2) for  $0 < \alpha < 1$  or  $m = 1$ .

### **5.3 Shifted Legendre Polynomials**

The shifted Legendre polynomials are well known Legendre polynomials which are shifted from  $[-1,1]$  to  $[0,1]$  by variable transformation  $\xi \rightarrow 2\xi - 1$ . We define shifted Legendre polynomials as:

$$\theta_i(\xi) = l_i(2\xi - 1), \quad (5.6)$$

where  $l_i$  denote the Legendre polynomials of degree  $m$  and satisfy,

$l_0(\xi) = 1, l_1(\xi) = \xi$  and,

$$l_{i+1}(\xi) = \frac{2i+1}{i+1} \xi l_i(\xi) - \frac{i}{i+1} l_{i-1}(\xi), \quad i = 1, 2, 3, \dots, \quad (5.7)$$

and satisfy orthogonality with respect to the weight function 1, *i.e.*,

$$\int_0^1 \theta_i(\xi) \theta_j(\xi) d\xi = \frac{1}{2i+1} \delta_{ij}, \quad (5.8)$$

where  $\delta_{ij}$  is Kronecker Delta function. Suppose  $X = L^2(\mathfrak{I})$  be the inner product space and inner product in this space is defined by,

$$\langle h_1 | h_2 \rangle = \int_0^1 h_1(\xi) h_2(\xi) d\xi, \quad (5.9)$$

and the corresponding norm is as follows,

$$\| h \|_2 = \left( \int_0^1 |h(\xi)|^2 d\xi \right)^{1/2}. \quad (5.10)$$

### 5.3.1 Function Approximation

Any function  $h(\xi)$  in  $L^2(\mathfrak{I})$  can be approximated as,

$$h(\xi) \approx \sum_{i=0}^R c_i \theta_i(\xi), \quad (5.11)$$

where,  $C$  and  $\theta(\xi)$  are vectors given by,

$$C = [c_0, c_1, \dots, c_R], \quad (5.12)$$

$$\theta(\xi) = [\theta_0(\xi), \theta_1(\xi), \dots, \theta_R(\xi)]. \quad (5.13)$$

Here,  $C$  denotes a vector of some suitable coefficients.

**Theorem 5.1 [86]** Let  $h(\xi)$  be a real sufficiently smooth function in  $L^2(\mathfrak{I})$  and  $h(\xi) \approx \sum_{i=0}^R c_i \theta_i(\xi)$  denotes the shifted Legendre expansion of  $h(\xi)$ , where

$C = [c_0, c_1, \dots, c_R]$  and,

$$c_i = (2i + 1) \int_0^1 h(\xi) \theta_i(\xi) d\xi, \quad (5.14)$$

then there exists a real constant  $\alpha$  satisfying,

$$\| h(\xi) - h_R(\xi) \|_2 \leq \frac{\alpha}{(R+1)! 2^{2R+1}}, \quad (5.15)$$

where,  $\alpha = \max\{ |h^{R+1}(\xi)| \mid \xi \in (0,1) \}$ .

## 5.4 Collocation Method for GFIDEs

In this section, we solve a new GFIDEs given by Eq. (5.1) with boundary condition mentioned by Eq. (5.2) using collocation approach. Collocation method is based on projection method where we choose a finite dimensional family of functions to approximate exact solution and then by applying collocation method we obtain an algebraic system of algebraic equations and further such systems can be solved using any standard method.

We now approximate function  $\gamma(\xi)$  by Eq. (5.11),

$$\gamma_R(\xi) \approx \sum_{i=0}^R c_i \theta_i(\xi). \quad (5.16)$$

Substitute the value of  $\gamma_R(\xi)$  in (5.1), we get,

$$(B_p^\alpha \gamma_R)(\xi) = (H \gamma_R)(\xi), \quad 0 < \alpha < 1, \quad (5.17)$$

$$\text{and } \gamma_R(0) = \gamma_0. \quad (5.18)$$

$$\text{or, } (B_P^\alpha(\sum_{r=0}^R c_i \theta_i))(\xi) = (H \sum_{i=0}^R c_i \theta_i)(\xi), \quad (5.19)$$

$$\sum_{i=0}^R c_i \theta_i(\xi) = \gamma_0. \quad (5.20)$$

We pick distinct node points  $\xi_k \in [0,1]$ , such that,

$$(B_P^\alpha(\sum_{i=0}^R c_i \theta_i))(\xi_k) = (H \sum_{i=0}^R c_i \theta_i)(\xi_k), \quad k = 0,1, \dots, R-1. \quad (5.21)$$

$$\text{And, } \sum_{i=0}^R c_i \theta_i(\xi_k) = \gamma_0. \quad (5.22)$$

Now, Eq. (5.1) is converted into Eq. (5.21)-(5.25) which is a system of equations in terms of unknowns  $\{c_i\}$  and it by solving using any standard method the approximate solution is obtained. For solving system of equations numerically, we use the Mathematica software.

### 5.4.1 Convergence Analysis

**Lemma 5.1** Let  $\gamma(\xi)$  be sufficiently smooth function in  $L^2(\mathfrak{I})$  and  $(\frac{d\gamma_R}{d\xi})$  be the approximation of  $\frac{d\gamma}{d\xi}$ . Assume that  $\frac{d\gamma}{d\xi}$  is bounded by a constant  $C$ , i.e.  $|\frac{d\gamma}{d\xi}| \leq C$ , then we have

$$\| \frac{d\gamma}{d\xi} - (\frac{d\gamma_R}{d\xi}) \|_2^2 \leq \left(\frac{C}{\pi}\right)^2 \frac{1}{R^2}. \quad (5.23)$$

Proof: Let,

$$\frac{d\gamma}{d\xi} = \sum_{i=0}^{\infty} c_i \theta_i(\xi). \quad (5.24)$$

Truncating it up to  $R-1$  level, we get,

$$\left(\frac{d\gamma_R}{d\xi}\right) = \sum_{i=0}^{R-1} c_i \theta_i(\xi). \quad (5.25)$$

From Eq. (5.23) and (5.24), we have,

$$\frac{d\gamma}{d\xi} - \left(\frac{d\gamma_R}{d\xi}\right) = \sum_{i=R}^{\infty} c_i \theta_i(\xi),$$

$$\left\| \frac{d\gamma}{d\xi} - \left(\frac{d\gamma_R}{d\xi}\right) \right\|_2^2 = \int_0^1 \left( \frac{d\gamma}{d\xi} - \left(\frac{d\gamma_R}{d\xi}\right) \right)^2 dx = \int_0^1 (\sum_{i=R}^{\infty} c_i \theta_i(\xi))^2 d\xi,$$

or,

$$\left\| \frac{d\gamma}{d\xi} - \left(\frac{d\gamma_R}{d\xi}\right) \right\|_2^2 = \sum_{i=R}^{\infty} \frac{c_i^2}{2i+1}. \quad (5.26)$$

$$c_i = (2i + 1) \int_0^1 \frac{d\gamma}{dx} \theta_i(\xi) d\xi,$$

$$c_i \leq (2i + 1) C \int_0^1 \theta_i(\xi) d\xi \leq (2i + 1) C \frac{\sin(i\pi)}{(i+i^2)\pi} \leq \frac{(2i+1)C}{(i+i^2)\pi}.$$

$$|c_i|^2 \leq \left( \frac{(2i+1)C}{(i+i^2)\pi} \right)^2. \quad (5.27)$$

Thus,

$$\sum_{i=R}^{\infty} \frac{c_i^2}{2i+1} \leq \sum_{i=R}^{\infty} \left( \frac{C}{\pi} \right)^2 \frac{2i+1}{((i+i^2))^2} = \left( \frac{C}{\pi} \right)^2 \frac{1}{R^2}. \quad (5.28)$$

## 5.4.2 Error Analysis

**Case 1: When  $\mathcal{G}$  is Linear.**

Let  $E_R(\xi) = \gamma(\xi) - \gamma_R(\xi)$  denote the error function of the approximate solution  $\gamma_R(\xi)$  to the exact solution  $\gamma(\xi)$  of Eq. (5.1).

Substituting the approximate solution in Eq. (5.1) we get,



$$(B_P^\alpha \gamma_R)(\xi) = (H\gamma_R)(\xi) = \varphi(\xi) + q(\xi)\gamma_R(\xi) + \int_0^\xi \rho(\xi, \eta)\mathcal{G}(\gamma_R(\eta))d\eta,$$

Subtracting above equation from Eq. (5.1) and rearranging the term we get,

$$q(\xi)(E_R(\xi)) = \int_0^\xi \rho(\xi, \eta) \left( \mathcal{G}(\gamma(\xi)) - \mathcal{G}(\gamma_R(\xi)) \right) d\eta - (B_P^\alpha(\gamma - \gamma_R))(\xi), \quad (5.29)$$

Since  $\mathcal{G}$  is linear, we have,

$$|q(\xi)E_R(\xi)| \leq \left| \int_0^\xi \rho(\xi, \eta)\mathcal{G}(E_R(\eta))d\eta \right| + |(B_P^\alpha(\gamma - \gamma_R))(\xi)|. \quad (5.30)$$

$$|q(\xi)E_R(\xi)| \leq Q \left| \int_0^\xi E_R(\eta)d\eta \right| + |(B_P^\alpha(\gamma - \gamma_R))(\xi)|.$$

where  $Q = \max \rho(\xi, \eta)$ .

Now, by Gronwall's inequality,

$$\| q(\xi)E_R(\xi) \|_2 \leq \| (B_P^\alpha(\gamma - \gamma_R))(\xi) \|_2. \quad (5.31)$$

$$\text{Now, } \| (B_P^\alpha(\gamma - \gamma_R))(\xi) \|_2 \leq \| T_1 \|_2 + \| T_2 \|_2. \quad (5.32)$$

where  $T_1 = r \int_0^\xi \omega_{1-\alpha}(\xi, \eta)\mathfrak{D}(\gamma(\eta) - \gamma_R(\eta))d\eta$  and  $T_2 = s \int_\xi^1 \omega_{1-\alpha}(\eta, \xi)\mathfrak{D}(\gamma(\xi) - \gamma_R(\xi))d\xi$ .

Since  $\omega_{1-\alpha}(\xi, \eta) \in L^2$ , then by Lemma 2.1 (Chapter 1) there exist constants  $\Lambda_1, \Lambda_2$  such that,

$$\| T_1 \|_2 \leq \Lambda_1 \| \mathfrak{D}(\gamma(\xi) - \gamma_R(\xi)) \|_2,$$

and

$$\| T_2 \|_2 \leq \Lambda_2 \| \mathfrak{D}(\gamma(\xi) - \gamma_R(\xi)) \|_2.$$

Thus,  $\| (B_P^\alpha(\gamma - \gamma_R))(\xi) \|_2 \leq \Lambda \| \mathfrak{D}(\gamma(\xi) - \gamma_R(\xi)) \|_2$ ,  $\Lambda = \Lambda_1 + \Lambda_2$ .

Using Lemma 5.1,

$$\| (B_P^\alpha(\gamma - \gamma_R))(\xi) \|_2 \leq \Lambda \left(\frac{C}{\pi}\right)^2 \frac{1}{R^2}. \quad (5.33)$$

From Eq. (5.31) and (5.33), we get,

$$\| q(\xi)E_R(\xi) \|_2 \leq \Lambda \left(\frac{C}{\pi}\right)^2 \frac{1}{R^2}. \quad (5.34)$$

Since  $q(\xi) \neq 0$ , therefore  $E_R(\xi) \rightarrow 0$  or  $\gamma(\xi) \rightarrow \gamma_R(\xi)$  as  $R \rightarrow \infty$ .

**Case 2: When  $\mathcal{G}$  is Nonlinear.**

Let  $\mathcal{G}$  satisfy the Lipschitz condition defined by,

$$|\mathcal{G}(\gamma_1(\eta)) - \mathcal{G}(\gamma_2(\eta))| \leq \mathcal{L}|\gamma_1(\eta) - \gamma_2(\eta)|, \quad (5.35)$$

where  $\mathcal{L}$  is constant independent of  $\gamma$ .

So by Eq. (5.29), we obtain,

$$|q(\xi)E_R(\xi)| \leq \int_0^\xi \mathcal{L}|\rho(\xi, \eta)| |E_R(\eta)| d\eta + |(B_P^\alpha(\gamma - \gamma_R))(\xi)|,$$

or,

$$|q(\xi)E_R(\xi)| \leq \mathcal{L} Q \left| \int_0^\xi |E_R(\eta)| d\eta \right| + |(B_P^\alpha(\gamma - \gamma_R))(\xi)|. \quad (5.36)$$

Now proceeding from Eq. (5.31), we obtain the result given by Eq. (5.34)

### 5.4.3 Error Estimate

Let  $E_R(\xi) = \gamma(\xi) - \gamma_R(\xi)$  denotes the error function of approximate solution  $\gamma_R(\xi)$  to the exact solution  $\gamma(\xi)$ . By substitution of  $\gamma_R(\xi)$  in Eq. (5.1), we have

$$(B_P^\alpha \gamma_R)(\xi) + Y_R(\xi) = \varphi(\xi) + q(\xi)\gamma_R(\xi) + \int_0^\xi \rho(\xi, \eta)\mathcal{G}(\gamma_R(\eta))d\eta, \quad (5.37)$$

with  $\gamma_R(0) = (\gamma_0)_R$ ,

where,  $(\gamma_0)_R$  is the approximated value of approximate solution  $\gamma_R(\xi)$  at  $\xi = 0$ , which depends on  $R$  and  $(\gamma_0)_R \rightarrow \gamma_0$  as  $R$  increases.

From Eq.(5.39), the perturbation function  $Y_R(\xi)$ , can be calculated as,

$$Y_R(\xi) = \varphi(\xi) + q(\xi)\gamma_R(\xi) + \int_0^\xi \rho(\xi, \eta)\mathcal{G}(\gamma_R(\eta))d\eta - (B_P^\alpha \gamma_R)(\xi).$$

Subtracting Eq. (5.39) from Eq. (5.5), we get

$$(B_P^\alpha E_R)(\xi) + Y_R(\xi) = \varphi(\xi) + q(\xi)E_R(\xi) + \int_0^\xi \rho(\xi, \eta)\mathcal{G}(E_R(\eta))d\eta,$$

or

$$(B_P^\alpha E_R)(\xi) = \varphi(\xi) + q(\xi)E_R(\xi) + \int_0^\xi \rho(\xi, \eta)\mathcal{G}(E_R(\eta))d\eta - Y_R(\xi), \quad (5.38)$$

with the initial condition  $E_R(0) = (E_0)_R$ .

Now error  $E_R(\xi)$  can be approximated by applying the proposed method described in section 5.4.

## 5.5 Numerical Results

To perform the numerical investigations, five test examples varying the convolution type kernels in B- operator are chosen. We also present the case where the GFIDEs takes the form of FIDEs discussed in literature. The numerical simulations are performed on the mathematical software Mathematica 10.

**Test example 5.1** Consider Eq. (5.1) with  $r = s = 1$  in B-operator,  $\alpha = 2/3$ ,  $\rho(\xi, \eta) = (\xi - \eta)^{-1/2}$ , kernel  $\omega_{1-\alpha}(\xi, \eta) = \frac{\{d+(1-d)(\xi-\eta)\}^{-\alpha}}{\Gamma(\alpha)}$ ,  $q(t) = 1$ , and

$$\varphi(\xi) = -\xi^2 - \frac{16\xi^{\frac{5}{2}}}{15} + \frac{9\xi^{\frac{4}{3}}}{2\Gamma(\frac{1}{3})} + \frac{3(1-\xi)^{1/3}(1+3\xi)}{2\Gamma(\frac{1}{3})}, \text{ with boundary condition } \gamma(0) = 0.$$

This has exact solution  $\xi^2$  for  $d = 0$ . This problem is solved using the proposed approach and numerical results with higher accuracy are obtained. Since the exact solution in this case is a second degree polynomial, therefore choice the basis functions up to  $R = 2$  would be sufficient to approximate the exact solution. The respective maximum absolute errors are also calculated and are shown in Table 5.1. The maximum absolute errors varying the number of polynomials ( $R = 2$  and  $R = 3$ ) are shown in Fig. 5.1. The numerical solutions are obtained varying the values of the parameter  $d = \frac{1}{8}, \frac{1}{16}, \frac{1}{32}$  and are displayed through Fig. 5.2. We observe that as  $d$  decreases the approximate solution approaches to the exact solution for  $d = 0$ . Fig 5.2 shows the approximate solution varying the value of the parameter  $d$ .

**Test example 5.2** Here, we choose Eq. (5.1) with  $r = s = 1$  in the B-operator,  $\alpha = 1/4$ ,  $\rho(\xi, \eta) = (\xi - \eta)^{-1/3}$ , kernel  $\omega_{1-\alpha}(\xi, \eta) = (1 - \alpha)(\xi - \eta)$ ,  $q(\xi) = 1$ , and

$\varphi(\xi) = \frac{17}{16} - \frac{3x}{2} - x^2 - \frac{x^3}{2} + \frac{3x^4}{8} - \frac{27}{440}x^{8/3}(11 + 9x)$ , with boundary condition  $\gamma(0) = 0$ .

The exact solution in this case becomes  $\xi^2 + \xi^3$ . We solve this problem for  $R = 2,3,4$  and obtained good approximate solution for  $R = 3$ . Maximum absolute errors for this case are listed in Table 5.1 for  $R = 2,3$  and are shown through Fig. 5.3 for  $R = 3,4$ .

Also we obtain and plot the approximate solution varying the value of  $\alpha = \frac{1}{5}, \frac{1}{6}, \frac{1}{7}, \frac{1}{8}$ . Fig. 5.4 ensures that the numerical solution approach to the exact solution as  $\xi^2 + \xi^3$  as  $\alpha$  increases.

**Test example 5.3** We take Eq. (5.1) with  $r = s = 1$  in the B-operator,  $\alpha = 3/4$ ,

$\rho(\xi, \eta) = (\xi - \eta)^{-1/2}$  kernel  $\omega_{1-\alpha}(\xi, \eta) = \frac{(\xi-\eta)^{-\alpha}}{\Gamma(\alpha)}$ ,  $q(t) = 1$ , and  $\varphi(\xi) = -e^\xi -$

$$e^\xi \sqrt{\pi} \operatorname{erf}(\sqrt{\xi}) + \frac{e^{\xi(1-\xi)^{\frac{1}{4}} \{ \Gamma(\frac{1}{4}) - \Gamma(\frac{1}{4}, \xi-1) \}}}{(\xi-1)^{\frac{1}{4}} \Gamma(\frac{1}{4})} + e^\xi \left\{ 1 - \frac{\Gamma(\frac{1}{4}, \xi)}{\Gamma(\frac{1}{4})} \right\},$$

with boundary condition  $\gamma(0) = 1$ .

This Test example has exact solution  $e^\xi$ . This equation is solved for  $R = 2,3,4,5$  and numerical solutions are obtained. The approximated solutions appear very close to the exact solution and as the number of Legendre basis functions are increased the error decreases. The maximum absolute errors for this example are presented through Fig. 5.5 and also shown in Table 5.2. Comparison of exact and numerical solution is shown in Fig. 5.6 with  $R = 5$ .

**Table 5.1** Maximum absolute errors for Test examples 5.1 and 5.2.

<b>R</b>	<b>Test example 5.1</b>	<b>Test example 5.2</b>
<b>2</b>	5.2041E-17	3.8524E-2
<b>3</b>	6.8082E-17	2.2898E-16

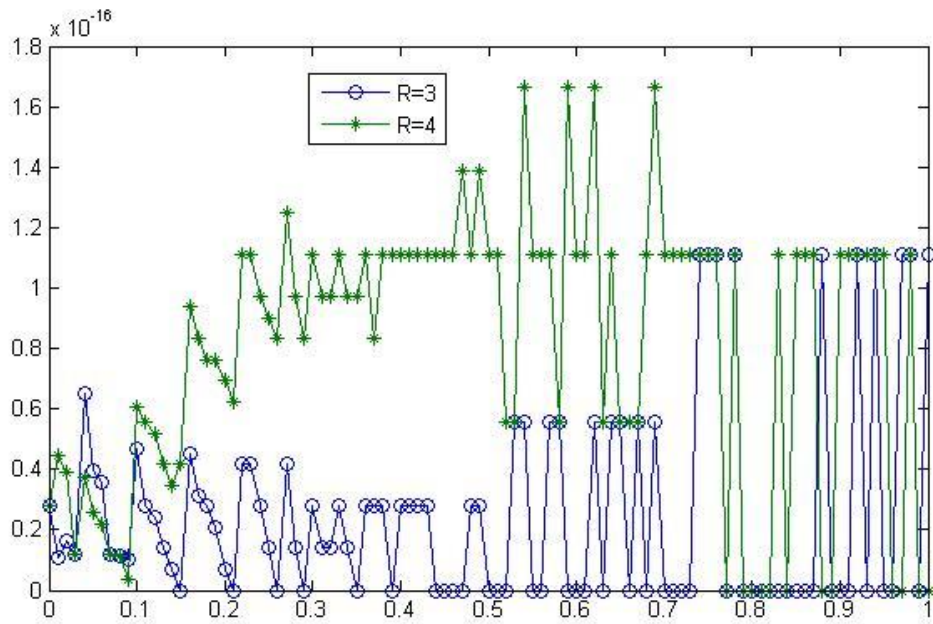


Fig. 5.1 Plot of Maximum absolute errors for Test example 5.1 for  $R = 3, 4$ .

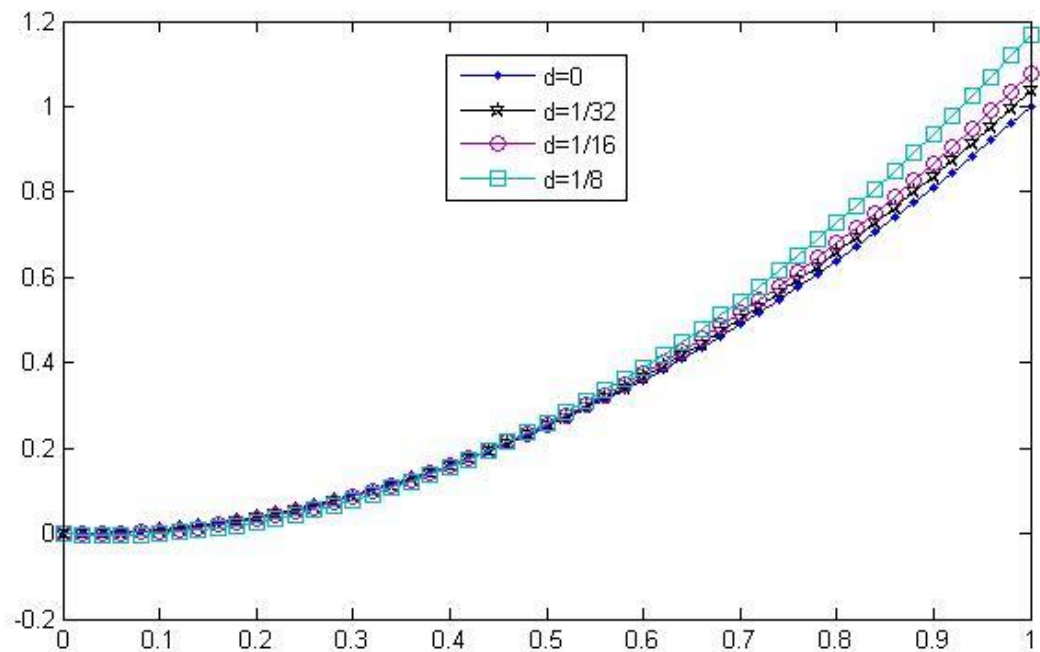


Fig. 5.2 Plot of approximate solutions for different values of  $d$  for Test example 5.1.

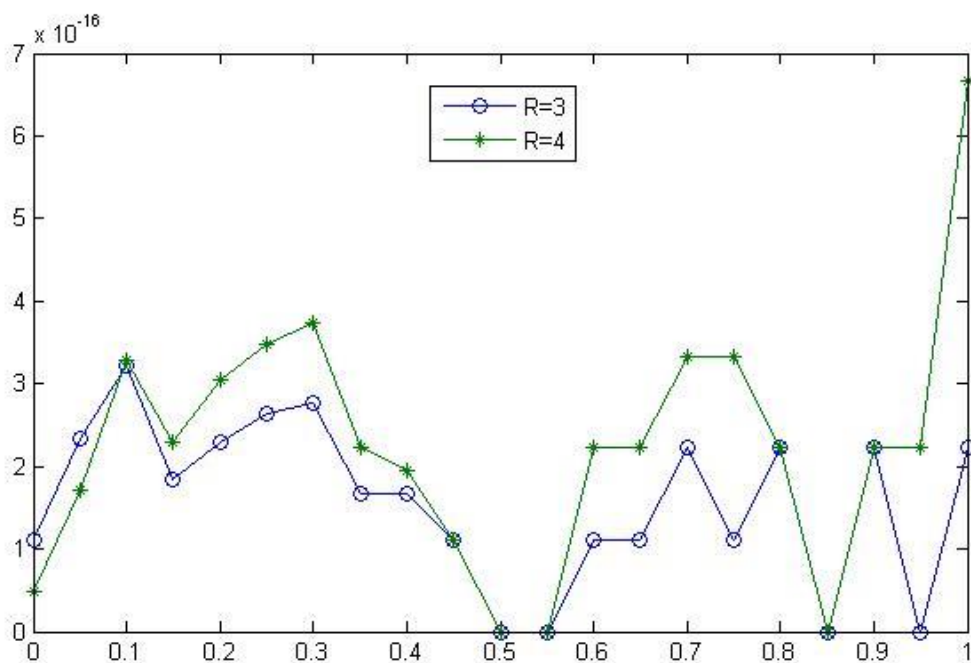


Fig. 5.3 Plot of maximum absolute errors for Test example 5.2 for  $R = 3, 4$ .

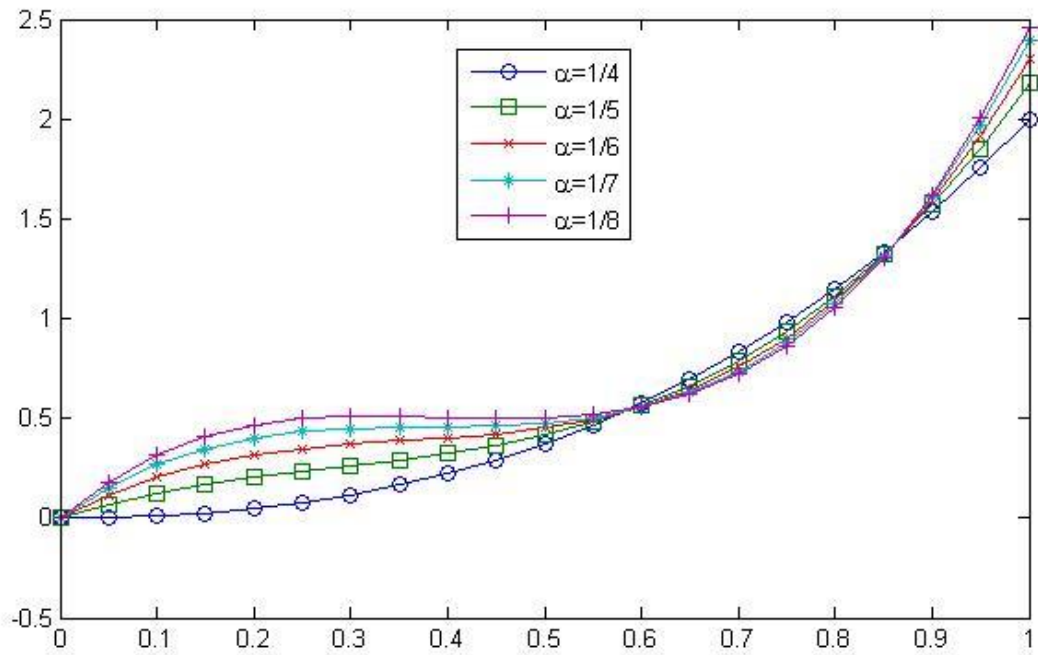


Fig. 5.4 Plot of approximate solutions for different values of  $\alpha$  for Test example 5.2.

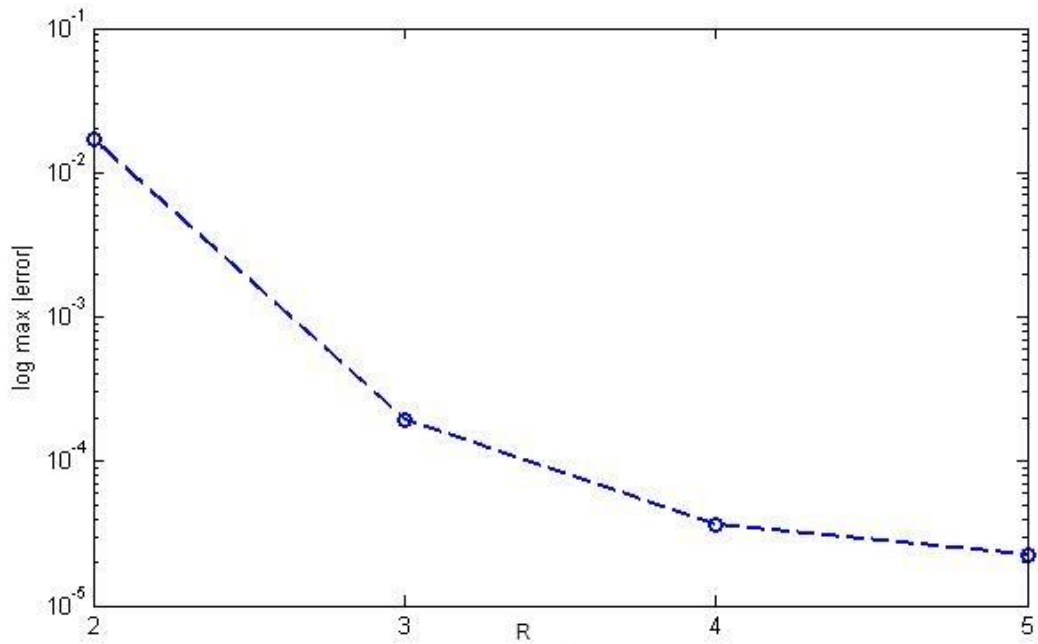


Fig.5.5 Error plot for Test example 5.3.



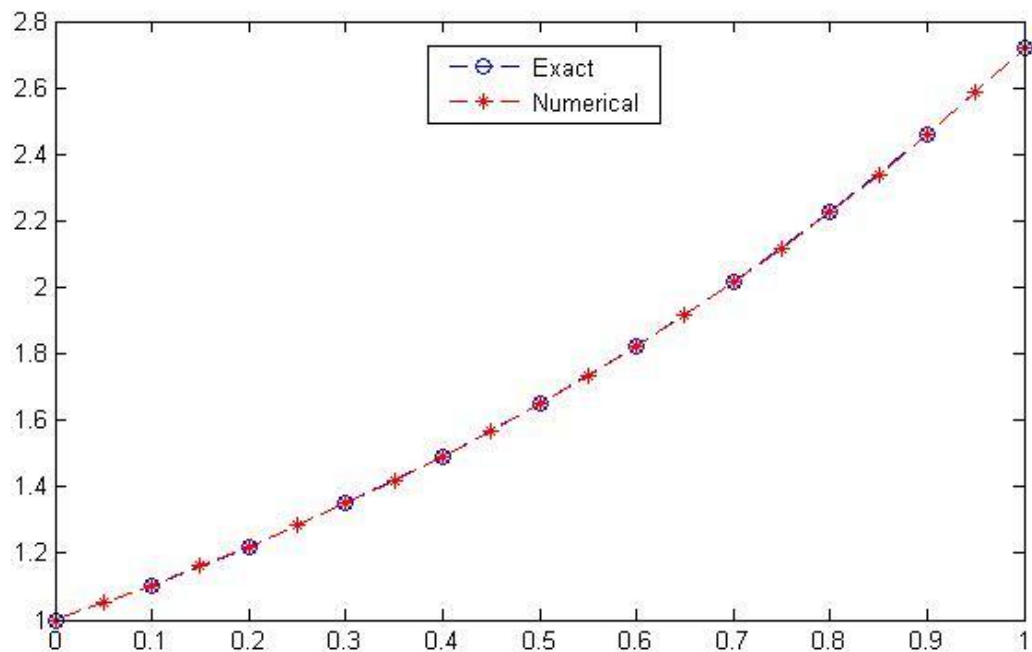


Fig. 5.6 Numerical versus exact solution for Test example 5.3 with  $R = 5$ .

**Test example 5.4** Consider Eq. (5.1) with  $r = 1, s = 1$  in the B-operator,  $\alpha = 1/2$ ,  $\rho(\xi, \eta) = (\xi - \eta)^{-1/2}$ , and kernel  $\omega_{1-\alpha}(\xi, \eta) = e^{-\alpha(\xi-\eta)}$ , with  $q(\xi) = 1$ ,

$$\text{and, } \varphi(\xi) = -e^{\xi} + \frac{2e^{-\xi/2}(-1+e^{3\xi/2})}{3\sqrt{\pi}} + \frac{-2e^{\xi}+2e^{\frac{1+\xi}{2}}}{\sqrt{\pi}} - e^{\xi}\sqrt{\pi}\text{Erf}[\sqrt{\xi}],$$

with boundary condition  $\gamma(0) = 1$ . In this case, the exact solution takes the form  $e^{\xi}$ . The presented approach is applied to this case and approximate numerical results are obtained with good accuracy. The calculated maximum absolute errors are shown in Table 5.2 and variations of maximum absolute errors are displayed through Figs. 5.7. Plot for different values of  $\alpha$  is shown in Fig.5.8.

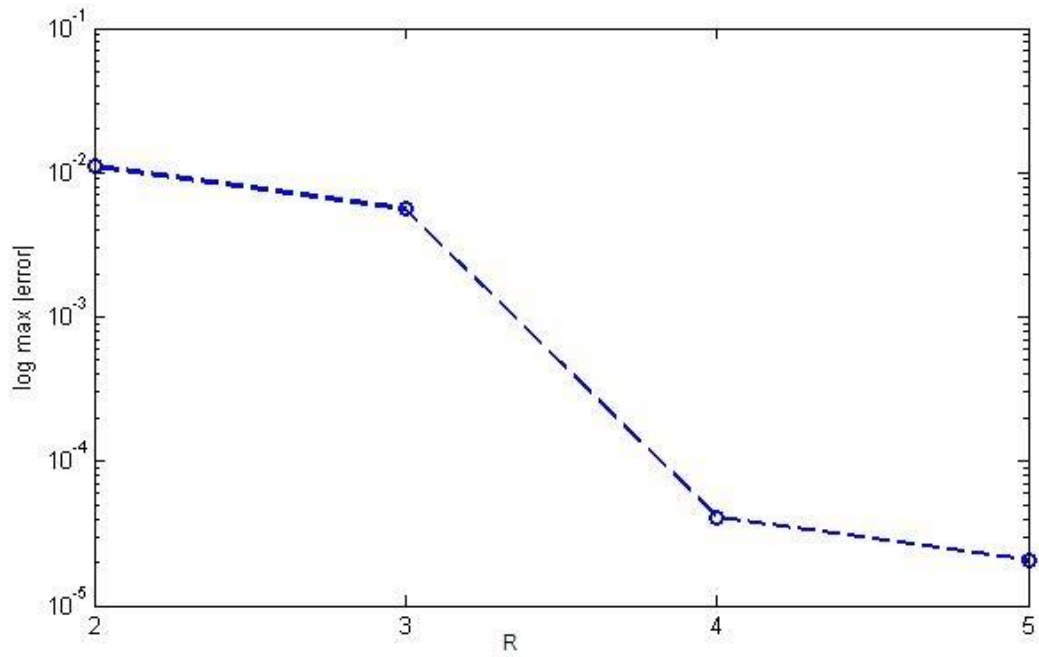


Fig. 5.7 Error plot for Test example 5.4.

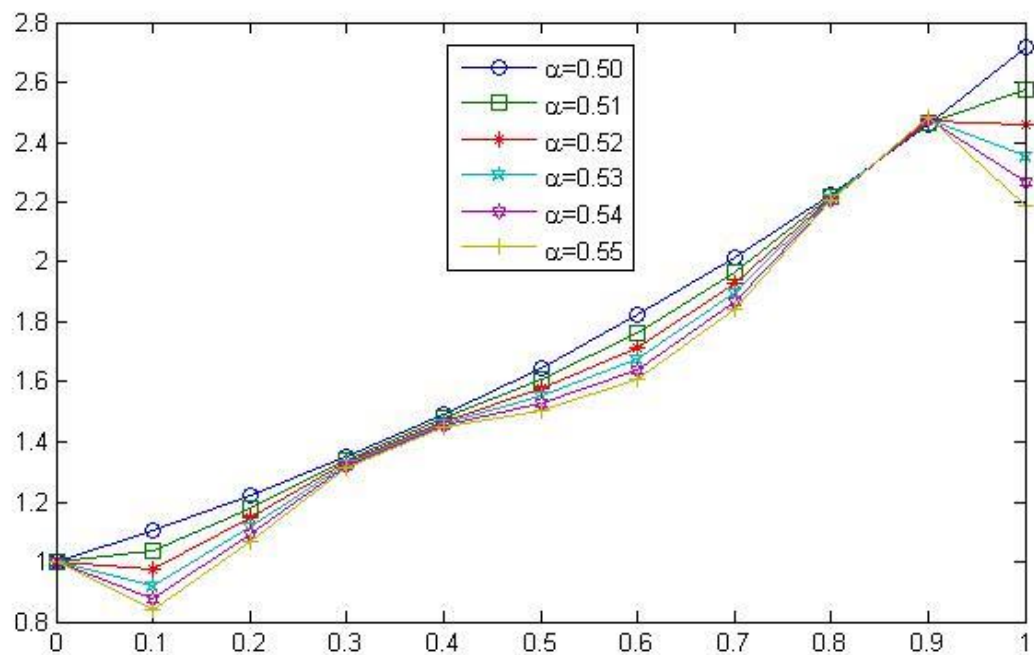


Fig. 5.8 Plot of approximate solutions for different values of  $\alpha$  for Test example 5.4.

**Test example 5.5 [81]** Consider the nonlinear case of Eq. (5.1) with  $r = 1, s = 0$  in the

B-operator,  $\alpha = 1/2$ ,  $\rho(\xi, \eta) = (\xi)^{1/2}$ , and kernel  $\omega_{1-\alpha}(\xi, \eta) = \frac{(\xi-\eta)^{-\alpha}}{\Gamma(\alpha)}$ , with

$$q(\xi) = 2\sqrt{\xi} + 2\xi^{3/2} - (\sqrt{\xi} + \xi^{3/2})\ln[1 + \xi],$$

$$\text{and, } \varphi(\xi) = -2\xi^{3/2} + \frac{2\text{ArcSinh}[\sqrt{\xi}]}{\sqrt{\pi}\sqrt{1+\xi}},$$

with boundary condition  $\gamma(0) = 0$ .

The exact solution of this problem is  $\ln(1 + t)$ . The methods discussed in section 5.4 has been studied on this problem and numerical results are obtained with good accuracy. The obtained numerical errors are illustrated in Fig. 9. and Table 2. Fig. 10 represents the plot of numerical and exact solution for  $R = 5$ . It is clear from Table 5.2 that numerical computational error converges to zero as the value of  $R$  increases.

**Table 5.2** Maximum absolute errors for Test examples 5.3, 5.4 and 5.5.

$R$	Test example 5.3	Test example 5.4	Test example 5.5
2	1.7019E-2	1.1104E-2	2.2891E-3
3	1.9441E-4	5.5713E-3	2.0455E-4
4	3.6687E-5	4.0970E-5	4.0699E-5
5	2.2674E-5	2.0755E-5	4.1765E-6

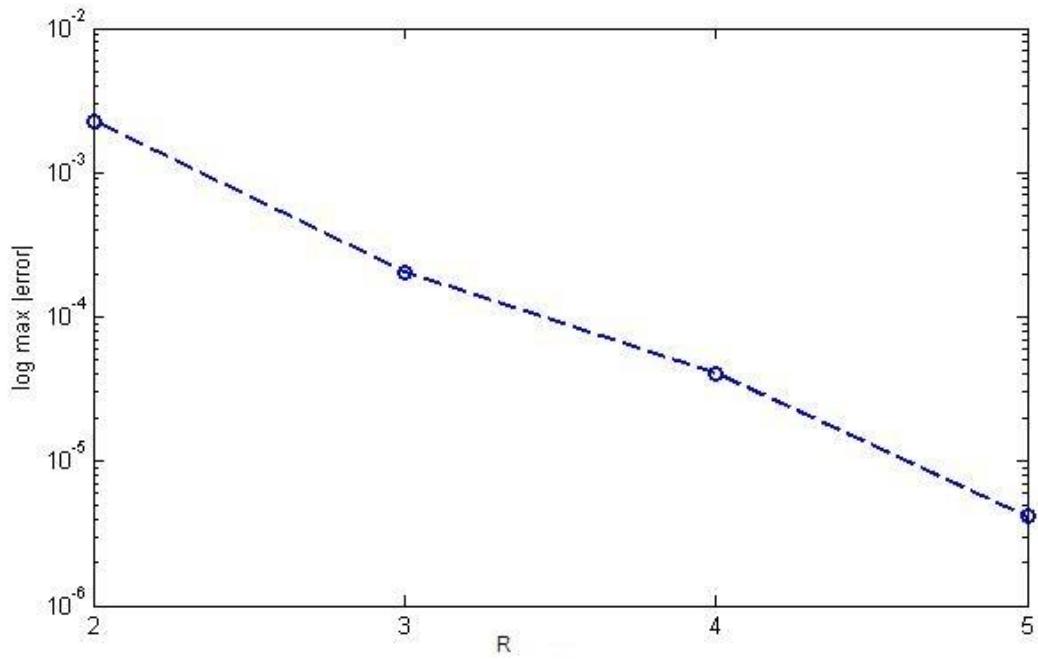


Fig. 5.9 Error plot for Test example 5.5 varying the number of polynomials  $R$ .

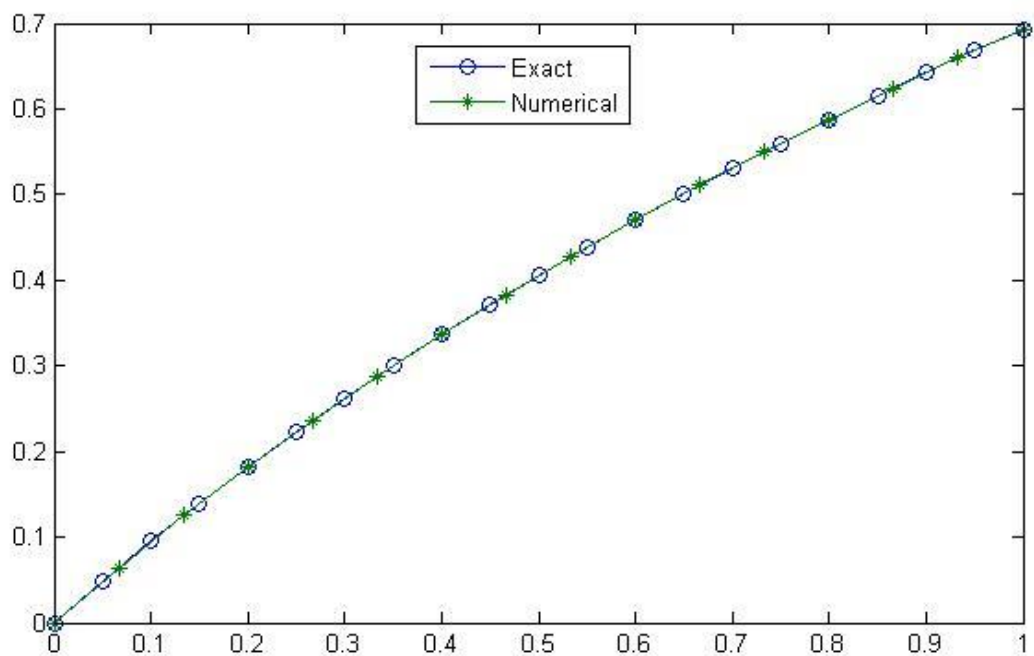


Fig. 5.10 Numerical versus exact solution for Test example 5.5 with  $R = 5$ .

## 5.6 Conclusion

A simple collocation approach is developed for the linear as well as nonlinear GFIDEs defined in terms of the B-operators. The convergence analysis of the collocation approach is also discussed and error bound of the approximation is obtained. Some numerical tests varying the kernel in the B-operator are considered and obtained simulations results are presented. Numerical results indicate that the presented approach for GFIDEs works well and obtains accurate results. It is observed that the proposed solution recovers the solutions of the FDIEs in special case and thus it could be considered as a general approach for solving FIDEs. We observe that good approximation of exact solution can be achieved with a less number of basis polynomials. The approximate method presented here could also be applied to similar problems defined in terms of the other fractional derivatives. This could be due to fact that the B-operators reduces to Riemann-Liouville fractional derivative and Caputo fractional derivatives and many other fractional derivatives defined in literature in special case.